The EMBO Journal (2008) 27, 244–252 | © 2008 European Molecular Biology Organization | All Rights Reserved 0261-4189/08
www.embojournal.org

THE
EMBO
JOURNAL

The post-rigor structure of myosin VI and implications for the recovery stroke

Julie Ménétrey[1,2,4], Paola Llinas[1,2,4], Jérome Cicolari[1,2], Gaëlle Squires[1,2], Xiaoyan Liu[3], Anna Li[3], H Lee Sweeney[3,*] and Anne Houdusse[1,2,*]

[1]Structural Motility, Institut Curie, Centre de Recherche, Paris, France; [2]CNRS UMR144, Paris, France and [3]Department of Physiology, University of Pennsylvania School of Medicine, Philadelphia, PA, USA

Myosin VI has an unexpectedly large swing of its lever arm (powerstroke) that optimizes its unique reverse direction movement. The basis for this is an unprecedented rearrangement of the subdomain to which the lever arm is attached, referred to as the converter. It is unclear at what point(s) in the myosin VI ATPase cycle rearrangements in the converter occur, and how this would effect lever arm position. We solved the structure of myosin VI with an ATP analogue (ADP.BeF_3) bound in its nucleotide-binding pocket. The structure reveals that no rearrangement in the converter occur upon ATP binding. Based on previously solved myosin structures, our structure suggests that no reversal of the powerstroke occurs during detachment of myosin VI from actin. The structure also reveals novel features of the myosin VI motor that may be important in maintaining the converter conformation during detachment from actin, and other features that may promote rapid rearrangements in the structure following actin detachment that enable hydrolysis of ATP.

The EMBO Journal (2008) **27,** 244–252. doi:10.1038/sj.emboj.7601937; Published online 29 November 2007
Subject Categories: structural biology
Keywords: directionality; lever arm; motility; myosin VI; unconventional myosin

Introduction

The generally accepted mechanism underlying myosin motor function is known as the swinging lever arm hypothesis (Holmes and Geeves, 2000; Sweeney and Houdusse 2004). According to this hypothesis, myosin motors generate movement while bound to actin via the rotation of a 'lever arm,' consisting of an extended alpha-helix to which multiple calmodulins or calmodulin-like light chains are bound (Figure 1A). The full extent of the force generating lever arm swing is known as the myosin powerstroke. The reverse movement, known as the recovery stroke, occurs once myosin has bound ATP and has dissociated from actin.

The lever arm itself is attached to a small subdomain of the motor called the converter, which determines the position of the lever arm (Figure 1A and B). The movements of the converter are in turn specified by coordinated rearrangements of two elements of the motor, the relay and the SH1-helix. The actions of these elements amplify motor domain rearrangements that are associated with changes in nucleotide state and actin binding.

The myosin powerstroke begins with binding to actin in a state known as the pre-powerstroke state, in which the ATP hydrolysis products are trapped, and ends in the rigor state in which the nucleotide pocket is empty (Holmes and Geeves, 2000; Sweeney and Houdusse 2004). The conformational changes between these states of the powerstroke involve sequential release of P_i and MgADP, which are coupled to movements of the myosin lever arm. The weakening of nucleotide affinity and eventual release of nucleotide involves relative movements of the nucleotide-binding elements, switch I and the P-loop (Coureux *et al*, 2003, 2004), which are attached to the upper 50-kDa (U50) and N-terminal (Nter) subdomains, respectively (see Figure 1A). Actin drives this decrease in nucleotide affinity by promoting formation of a high-affinity actin-binding interface by closing of a cleft (actin-binding cleft) that lies between two subdomains of the myosin motor, known as the upper and lower 50-kDa subdomains (U50 and L50; see Figure 1A). These coordinate translocations within the motor domain, which drive the swing of the lever arm, are accommodated by relieving a distortion in the seven-stranded beta-sheet that is seen in the non-actin-bound states of myosin (Coureux *et al*, 2004; Yang *et al*, 2007). This beta-sheet, with its associated loops and connectors, has been termed the transducer (Coureux *et al*, 2004) and is depicted in Figure 1A.

The powerstroke is terminated when ATP binds to myosin via the P-loop and switch I, distorting the beta-sheet and causing an opening of the actin-binding cleft. These changes result in the formation of what is known as the post-rigor state of the motor (Coureux *et al*, 2004; Sweeney and Houdusse, 2004). In plus-end-directed myosins, the formation of this state, which rapidly detaches from actin, involves little movement of the lever arm so as not to reverse the powerstroke before detachment from actin.

Once myosin dissociates from actin, a further rearrangement of the motor that involves the nucleotide-binding element, switch II (Figure 1A), promotes hydrolysis of ATP, and is concomitant with a repriming of the lever arm to its pre-powerstroke position. This recovery stroke has been extensively modeled for myosin II (Fischer *et al*, 2005; Koppole *et al*, 2006).

The most unusual feature of myosin VI is that unlike all other characterized classes of myosin, it moves toward the

*Corresponding authors. HL Sweeney, Department of Physiology, University of Pennsylvania School of Medicine, A700 Richards Bldg, 3700 Hamilton Walk, Philadelphia, PA 19104-6085, USA. Tel.: +1 215 898 8727; Fax: +1 215 573 2273; E-mail: Lsweeney@mail.med.upenn.edu or A Houdusse, Structural Motility, Institut Curie CNRS, UMR144, 26 rue d'Ulm, 75248 Paris cedex 05, France. Tel.: 33 1 42 34 63 95; Fax: 33 1 42 34 63 82; E-mail: Anne.Houdusse@curie.fr
[4]These authors contributed equally to this work

Received: 14 September 2007; accepted: 6 November 2007; published online: 29 November 2007

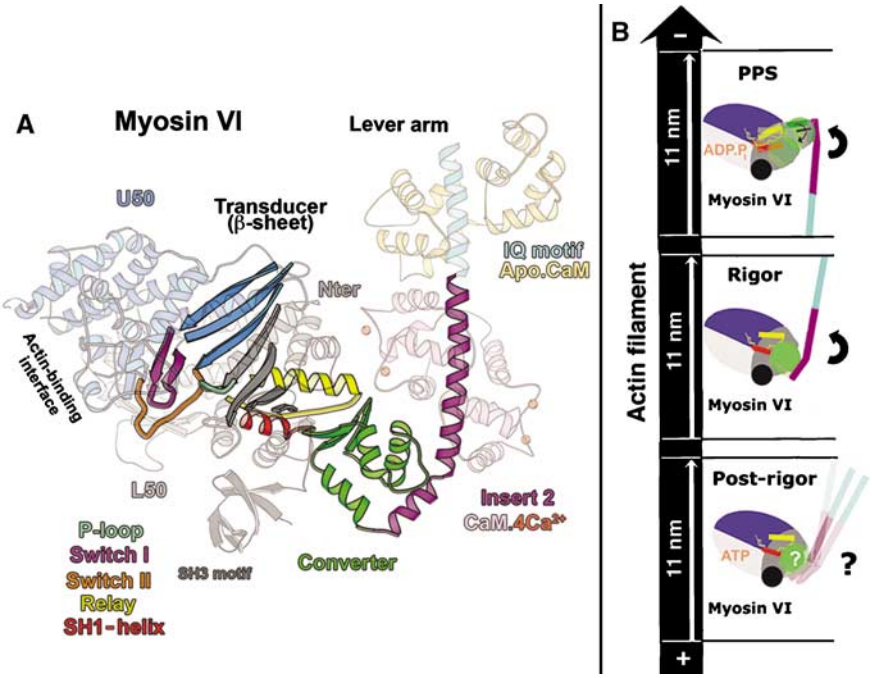

Figure 1 Important features of the myosin VI motor. (**A**) The different elements of the myosin VI motor are shown in the rigor-like myosin VI structure (Ménétrey *et al*, 2005). The motor domain is composed of four subdomains (Nter, U50, L50 and the converter). The converter (green) is the most mobile of these and is directly linked to the lever arm. In myosin VI, the converter interacts with a unique inserted structural element (insert 2; purple). This redirects the lever arm in the opposite direction from plus-end myosins. The central beta-sheet (gray and blue) is the major component of the transducer, which can adopt differently twisted conformations depending on the nucleotide- and actin-binding states of the motor. There are three nucleotide-binding elements: P-loop, switch I and switch II. Rotation of the converter is controlled by the rearrangements of the relay (yellow) and the SH1-helix (red). (**B**) Diagram illustrating the converter (green) and the lever arm (purple for the insert 2-CaM-binding region and cyan for the IQ-CaM) position in three states of the myosin VI motor cycle. The motor domain is composed of an SH3 domain (black ball) and four subdomains (N-terminal (Nter, gray), upper 50 kDa (U50, blue), lower 50 kDa (L50, light gray) and converter). The relay (yellow) and SH1-helix (red) are two connectors of the motor that direct the rotation of the converter. The powerstroke corresponds to the large (11 nm) movement of the lever arm between the pre-powerstroke (PPS, 2V26) and rigor state (2BKH), during which the converter both rotates and alters its conformation. ATP binding in the rigor state induces rearrangements in the motor to detach the motor from actin and produce the post-rigor state. To optimize the powerstroke, no reversal of the lever arm movement should occur upon ATP binding and myosin detachment from actin. However, it is not clear that this can be accomplished for myosin VI, since it is unclear what happens to the converter conformation and lever arm position following ATP binding.

pointed (−) end of actin filaments (Wells *et al*, 1999). This allows it to play a number of unique cell biological roles (Sweeney and Houdusse, 2007). The reversal of direction is due to the repositioning of the lever arm by insert 2, a myosin VI-specific insertion, which is a calmodulin-binding structural extension of the converter subdomain (Ménétrey *et al*, 2005; Figure 1A). Insert 2 is solely responsible for the reversal of myosin VI directionality, as its removal causes myosin VI to become a plus-end-directed motor on actin (Bryant *et al*, 2007; Park *et al*, 2007). However, in order to generate its measured powerstroke of 11–12 nm (Rock *et al*, 2005), myosin VI adopts a novel conformation of its converter in its pre-powerstroke state, and likely during the initial phases of the powerstroke (Ménétrey *et al*, 2007). In rigor, the converter assumes the conformation that has been seen in all other myosin structures, which is stabilized by interactions with the N-terminal subdomain. Furthermore, the pre-powerstroke converter conformation is incompatible with the rigor structure due to steric clashes between the converter and N-terminal subdomain (Ménétrey *et al*, 2007).

It is unclear at what point in the powerstroke the converter rearranges to form the conventional conformation that is seen in rigor, and at what point following rigor (recovery stroke) it returns to the pre-powerstroke conformation. To begin to understand at what steps in the cycle that the myosin VI converter rearrangements occur, we have solved the structure of the motor with an ATP analogue bound in a state that has previously been referred to as post-rigor (Coureux *et al*, 2004). This is the state that is created following ATP binding to myosin in the rigor state on actin. Rearrangements that allow the elements of the nucleotide pocket to strongly coordinate nucleotide concomitantly open the actin-binding cleft causing dissociation of the myosin from actin (Coureux *et al*, 2004; Sweeney and Houdusse, 2004). To optimize the powerstroke of any myosin, it is important that there be little or no lever arm motion associated with ATP-binding and detachment from actin. We have proposed that interactions between the N-terminal subdomain and the rigor conformation of the myosin VI converter are critical to maintaining the converter conformation (Ménétrey *et al*, 2007). However, it is not clear if those interactions can be maintained in the post-rigor state based on structures that have been obtained to date, and therefore whether or not the myosin VI lever arm position is maintained during detachment from actin. Thus, either there is yet another conformation of the myosin VI converter in

post-rigor, or the myosin VI motor has additional adaptations to allow maintenance of the rigor converter conformation in the post-rigor state (see Figure 1B).

Results

The post-rigor structure of the myosin VI is similar to plus-end myosins

The post-rigor state of myosin, which corresponds to the ATP state of the motor, can be induced by the binding of ATP analogues such as MgAMPPNP and MgADP.BeF_3 (Fisher *et al*, 1995; Gulick *et al*, 1997). Our initial attempts at crystallization of the post-rigor state of myosin VI used truncated myosin VI constructs with either the motor domain with its full lever arm (two calmodulins bound to insert 2 and the IQ motif, MD-IQ construct), or the motor domain with only the insert 2 calmodulin bound ($MD^{insert\ 2}$ construct). However, we failed to obtain crystals with either MgAMPPNP or MgADP plus BeF_3 trapped at the nucleotide-binding site with either construct. Based on our previous observation that removal of insert 1 (near the nucleotide-binding pocket) increases nucleotide affinity (Ménétrey *et al*, 2005; Sweeney *et al*, 2007), we attempted to crystallize $MD^{insert\ 2}$ with insert 1 removed ($MD^{insert\ 2,}\ \Delta^{insert\ 1}$), with MgADP.$BeF_3$ trapped at the nucleotide-binding site. This myosin VI construct crystallized in a state that is nearly equivalent to the post-rigor state of other myosins, as shown in Figure 2 and Table I. The amazing similarity of the structure with other post-rigor state structures for the subdomain positions, the transducer conformation as well as the nucleotide-binding site geometry allows us to identify this new structure as the post-rigor state of myosin VI. The crystals diffracted up to 2.4 Å, allowing determination of the myosin VI post-rigor structure (see Table II for statistics on data collection and refinement.)

As shown in Figure 2B, the myosin VI actin-binding cleft is open in the post-rigor structure, and the overall motor domain conformation as well as the nucleotide-binding site are similar to that of myosin V or myosin II in the post-rigor state (Fisher *et al*, 1995; Gulick *et al*, 1997; Houdusse *et al*, 2000; Coureux *et al*, 2004). This motor domain conformation greatly differs from the rigor-like state (Figure 2B). As described for plus-end myosins, during the transition from rigor to post-rigor, the major coordinated movements in the motor domain are induced by the distortion of the seven-stranded beta-sheet of the transducer (Coureux *et al*, 2004; Yang *et al*, 2007). While only the P-loop can participate in nucleotide binding in the rigor state, transducer rearrangements allow both nucleotide-binding elements, P-loop and Switch I, to simultaneously coordinate ATP in the post-rigor state. These rearrangements cause the opening of the actin-binding cleft, drastically reducing the affinity of the actin interface, resulting in the dissociation of the motor from actin. In conclusion, ATP binding to the motor domain of this minus end motor induces nearly identical rearrangements as those previously described for plus-end myosins. These structural rearrangements provide the structural basis for the reciprocity between actin- and ATP-binding affinities of myosin motors (Coureux *et al*, 2004; Yang *et al*, 2007).

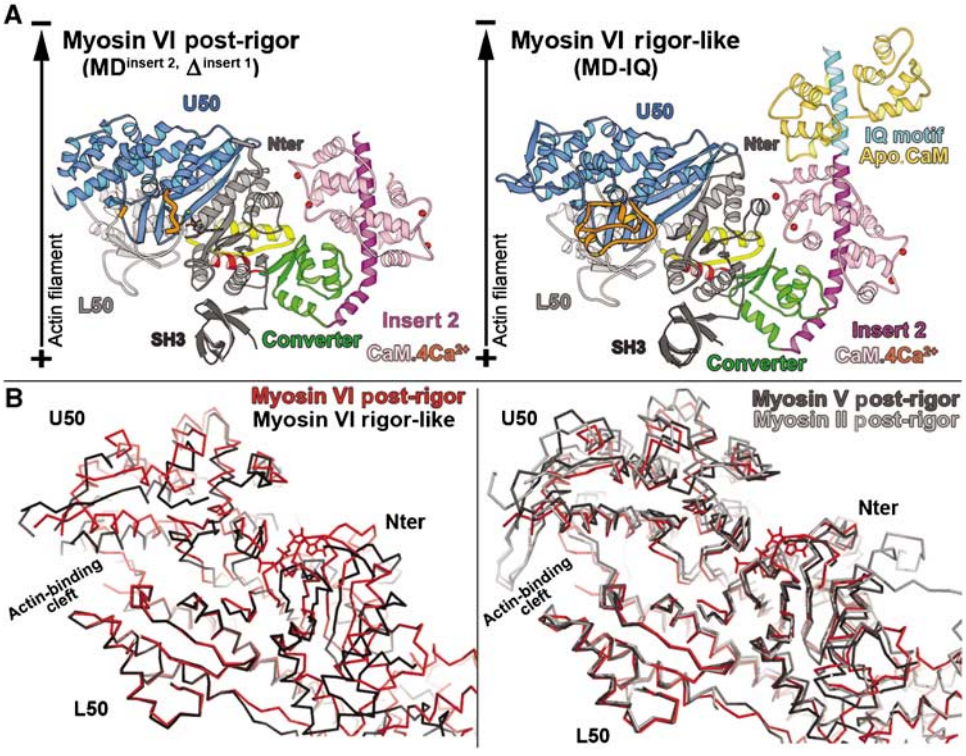

Figure 2 The post-rigor state of myosin VI. (**A**) The myosin VI post-rigor structure is compared to that in the rigor-like state (right). The motors are oriented as if they are bound to a vertical actin filament (black arrow). Note the position of the lever arm, which is very similar in the rigor-like and post-rigor states. (**B**) On the left, porcine myosin VI in the post-rigor state (red) is compared with the myosin VI rigor-like state (black) after superposition of the L50 subdomains. Note the difference in the position of the Nter and U50 subdomains. The actin-binding cleft is more open in the post-rigor state (red) compared with the rigor-like state (black). On the right, three different post-rigor state structures are superimposed (chicken myosin V in black, *Dictyostelium* myosin II in gray and porcine myosin VI in red). Note that the positions of their subdomains are quite similar.

Table I Actin-binding 50-kDa cleft orientation and closure in different myosin VI states

Isoform	Cleft orientation angle (deg) between Cα of Nter residues 120, 160 and		Cleft closure distance (Å), at the indicated location of the cleft, between Cα of the indicated U50 and L50 kDa residues			
	U50 kDa residue 418	U50 kDa residue 598	Far outer cleft (near actin) 361–536	Outer cleft (strut) 418–598	Inner cleft 239–467	Far inner cleft (switches) 199–463
Rigor-like state						
Myosin VI (2BKH)	129	118	18.2	8.3	11.1	10.3
Myosin V (1OE9)	129	120	13.2	7.2	9.6	7.9
Squid (2OVK)	127	117	13.2	7.8	9.8	7.3
Placo catch (2OS8)	126	115	14.3	8.4	12.9	10.4
Post-rigor state						
Myosin VI (2VAS)	148	129	21.7*	13.2	14.7	11.6
Myosin V (1W7J)	155	133	20.7	14.2	16.2	12.9
Squid (2OY6)	150	129	20.1	14.4	16.1	13.4
Argo catch (2OTG)	147	128	20.9	13.3	16.5	13.8
Pre-powerstroke state						
Myosin VI (2V26)	149	132	22.1	11.8	12.3	8.6
Argo striated (1QVI)	155	134	22.9	13.3	11.8	8.8

L50, lower 50-kDa subdomain; Nter, N-terminal; U50, upper 50-kDa subdomain.
Myosin VI residues used for measurements are equivalent to those used for squid from Yang *et al* (2007). 'Placo' indicates sea scallop myosin II and 'Argo' indicates bay scallop myosin II. (*) This value was measured using a modeled position of residue 361. This residue is indeed absent in the myosin VI post-rigor structure. The model was easily obtained using a superimposition of the U50 kDa subdomain of the myosin VI rigor-like structure (2BKH).

Table II Data collection and refinement statistics

MD $^{(\text{insert 2, }\Delta^{\text{insert 1}})}$	
Data collection	
Space group	$P2_12_12_1$
Cell dimensions	
a, *b*, *c* (Å)	73.42, 100.47, 174.07
Resolution (Å)	49.0–2.4 (2.53–2.40)
R_{mean}	10.4 (40.8)
$I/\sigma I$	6.6 (1.9)
Completeness (%)	100 (100)
Redundancy	8.2 (8.3)
Refinement	
Resolution (Å)	2.4
No. of reflections	51 212
R_{work}/R_{free}	21.7/25.5
No. of atoms	
Protein	7025
Heterogen	36
Water	154
Overall mean *B*-value (Å^2)	31.35
R.m.s. deviations	
Bond lengths (Å)	0.017
Bond angles (deg)	1.558

Data were collected from a single crystal. Values in parentheses are for the highest-resolution shell.

The rigor converter conformation is maintained in the post-rigor state

As shown in Figure 2A, this myosin VI post-rigor structure positions the lever arm in an orientation that is very close to that found for the lever arm in the rigor-like state. This is made possible by the converter maintaining its rigor conformation, which is illustrated in detail in Figure 3. Even the specific contacts seen between the insert 2-CaM and the converter in the rigor-like structure are maintained in the post-rigor state (Figure 4). As seen for plus-end myosins, important rearrangements in the transducer upon opening of the actin-binding cleft affect the conformation of the relay and SH1-helix, and thus the relative orientation of the L50 and converter subdomains. These differences between the rigor and post-rigor states create an $\sim 40^\circ$ difference in the orientation of the last helix of the converter, but this component is mostly perpendicular to the actin helix. Interestingly, insert 2, which redirects the lever arm of myosin VI, compensates for this difference such that at the end of insert 2, the lever arm position (measured at residue E815) is only 8 Å apart in the two states. Thus only limited movement of the lever arm would occur during ATP-driven detachment of myosin VI from actin.

Interactions of the converter with the N-terminal subdomain are maintained

In myosin V, the interactions between the converter and N-terminal subdomains differ in rigor compared with post-rigor, while the interface between the converter and the relay is nearly identical in the two structures (Coureux *et al*, 2004). The reverse occurs in myosin VI, likely to help maintain the rigor conformation of the converter, which is stabilized by its interactions with the N-terminal subdomain (Ménétrey *et al*, 2007). Depicted in Figure 3B and C are the maintenance of interactions between the myosin VI converter and the N-terminal subdomain in the post-rigor state, as they exist in the rigor-like state. Note that the pre-powerstroke conformation of the converter is incompatible with this structure (as it is with the rigor-like structure), since it would generate steric clashes between the converter and the N-terminal subdomain (Figure 3D). The converter/N-terminal subdomain interactions found in both rigor and post-rigor are mediated by the C63-L68 loop of the N-terminal subdomain, which interacts with the first and last helices of the converter, as well as with the first strand of the beta-sheet. As we

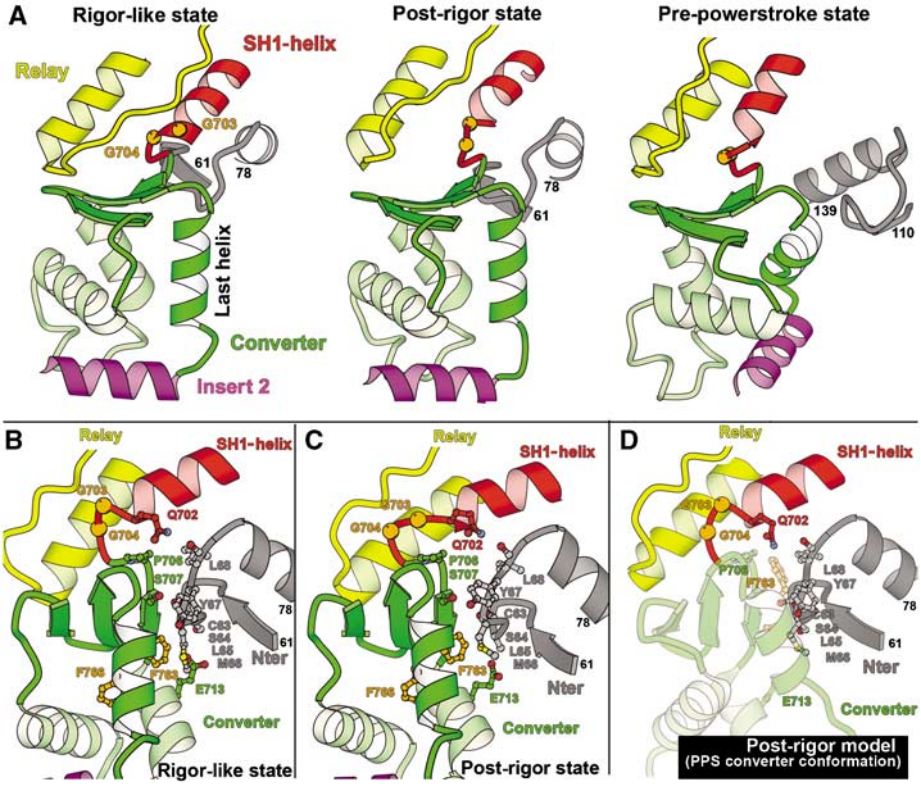

Figure 3 The converter conformation of myosin VI. (**A**) The converter conformation of myosin VI is unchanged between the rigor-like state and the post-rigor state. Note also that the converter interacts with the same N-terminal subdomain (gray) residues in these two states. In contrast, a novel folding of the converter drastically changes the orientation of the helices in the pre-powerstroke state (Ménétrey *et al*, 2007). Also, a different region of the N-terminal subdomain interacts with the converter. This novel conformation results in a reorientation of insert 2 and thus of the myosin VI lever arm in this state. (**B, C**) In the rigor-like state (B) and in the post-rigor state (C), the converter makes similar interactions with the C63-L68 loop of the N-terminal subdomain. (**D**) Depicted is a model that demonstrates that the pre-powerstroke conformation of the converter is incompatible with the post-rigor structure, as it would create major steric clashes with the N-terminal subdomain region.

previously speculated, these interactions are likely important for maintaining the rigor conformation of the converter (Ménétrey *et al*, 2007), and now appear to be equally important in post-rigor.

Alterations in the relay–converter interface

In order to maintain the interactions between the converter and the N-terminal subdomain, myosin VI slightly alters the position of the relay relative to the converter in the post-rigor state as compared with both its rigor-like and pre-powerstroke states, and indeed as compared with other myosin structures (see Figure 5A and B). Both the orientation of the relay helix and the position of the following loop differ such that the location of most residues differs by 5 Å in the two states. Interestingly, this accommodation does not involve the loss of any interactions between the relay and the converter (see Figure 5C and D). The relay can thus play its role in maintaining the converter connections to the motor domain. In myosin VI, a small translocation or sliding of the relay might however be important to help maintain the interactions of the converter with the N-terminal subdomain. Adaptations of the myosin VI relay sequence—such as the absence of a tryptophan at the tip of the relay (V503 in myosin VI, W501 in *Dictyostelium* myosin II and W484 in myosin V)—is likely important to allow sliding on hydrophobic patches between the relay and the surface of the converter.

A further illustration of the mobility surrounding the relay is the fact that two crystal forms were obtained for the myosin VI post-rigor state (Supplementary Figure 1; Supplementary Table I; Supplementary data). These two structures differ only by a small movement at the end of the SH1-helix. This movement, made possible by two adjacent glycines found at the end of the SH1-helix, allows the relay loop to become mobile in one of the crystals (Supplementary Figure 1). Note that a disordered relay loop has also been described in the post-rigor state of *Dictyostelium discoideum* myosin II. Differences in the sequence of the SH1-helix of myosin VI, as compared with plus-end myosins, may further increase flexibility in the connection of the converter to the motor domain. Also note that the cavity occupied by the SH1-helix is larger in myosin VI than in other characterized myosins. This is due to a difference in the conformation of the first two strands of the transducer beta-sheet (residues Y89–L94). These differences in the myosin VI sequences found in the relay, the SH1-helix and the N-terminal subdomain surface facing the SH1-helix may be important for this reverse motor to control the reorientation of its lever arm upon the recovery stroke.

Loss of interactions between the end of switch II and the L50 subdomain

An intriguing and unexpected feature of the post-rigor structure is a movement of the end of switch II (residues F460–F463) away from the lower 50-kDa subdomain by ~2.5 Å.

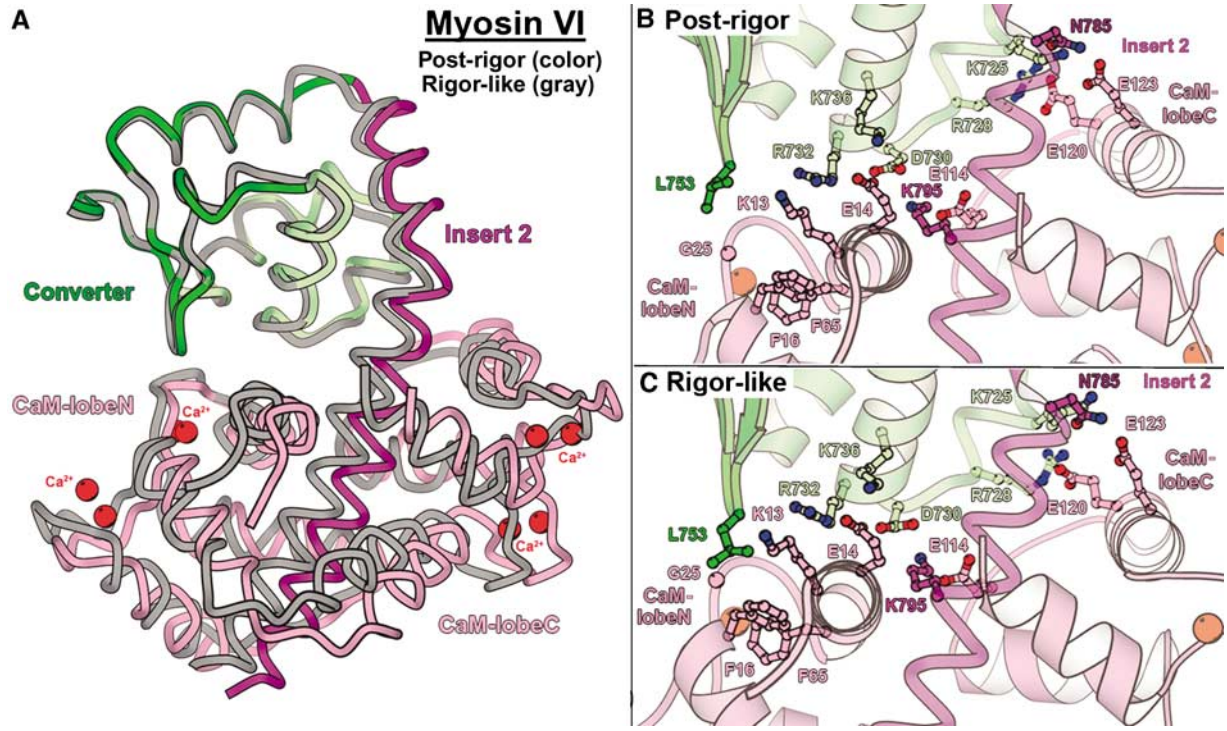

Figure 4 The Ca^{2+}-calmodulin bound to insert 2 interacts similarly with the converter in the rigor-like and post-rigor states. (**A**) An overall view of the converter/insert 2 region allows visualization of the similarity of the conformation of insert 2 and the position of the bound Ca^{2+}-calmodulin in these two states. (**B, C**) Details of the interface between the converter and the calmodulin are shown. Most of the interactions involved in this interface are found both in the (B) post-rigor and (C) rigor-like structures. Note that the interface is rather wide, involving both lobes of calmodulin. Note also that many of the interactions involve salt bridges.

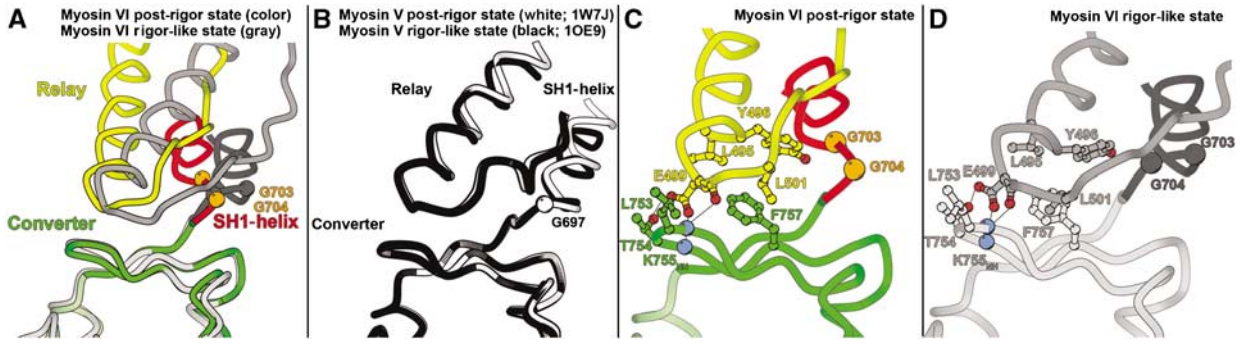

Figure 5 The relay–converter interface undergoes sliding on hydrophobic patches. (**A**) Comparison of the relay converter interactions in myosin VI post-rigor (color) and rigor-like (gray) states. Note the difference in the overall position and orientation of the relay in these two states. (**B**) In contrast, the relay of myosin V adopts the same position in the post-rigor (white) and rigor-like (black) states. (**C, D**) Despite the difference in the relay orientation, the interactions between the relay and the converter are similar in both the post-rigor (C) and rigor (D) states of myosin VI.

Such a movement has not been seen in other myosins and may be a class-specific adaptation. It results in the loss of seven highly conserved interactions between switch II and the lower 50-kDa subdomain, as illustrated in Figure 6. In all myosin structures described so far, the beginning of switch II (D456–F460 in myosin VI) is relatively free and adopts distinct conformations depending on the nucleotide state. After a bend at the fifth residue, the second part of switch II (F460–N466 in myosin VI) is oriented parallel to the L50 subdomain surface and interacts strongly with it in all the myosin structures seen prior to the post-rigor state of myosin VI. These conserved interactions are thought to be very important to couple and transmit the rearrangements occurring at the beginning of switch II into directed movement of the L50 subdomain, relative to the nucleotide-binding site. In the pre-powerstroke state, an important salt bridge interaction between switch I and the second part of switch II must occur to allow closure of the actin-binding cleft near the nucleotide, which is essential for nucleotide hydrolysis (Supplementary Figure 2; Fisher *et al*, 1995; Furch *et al*, 1999; Koppole *et al*, 2006). (For myosin VI, this occurs between residues E461 of switch II and R205 of switch I.) Note that in the myosin VI post-rigor state, the second part of switch II makes three hydrogen bonds with switch I and the P-loop, but these differ from the interactions that occur in the pre-powerstroke state. For example, the salt bridge formed by

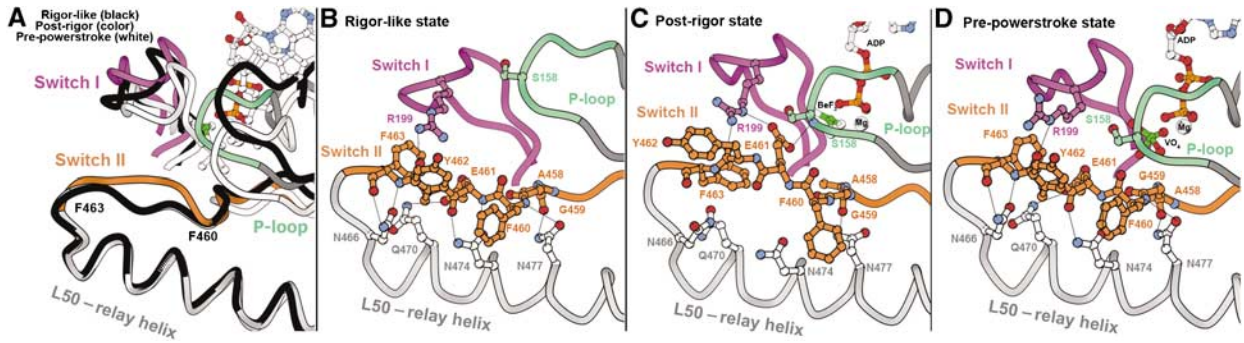

Figure 6 Mobility of switch II in the post-rigor state of myosin VI. (**A**) The conformation of switch II between residues F460 and F463 in the myosin VI post-rigor state (orange) differs by up to 2.5 Å from that adopted in the rigor-like state (black), the pre-powerstroke state (white) or in post-rigor states of other myosins (Fisher *et al*, 1995; Houdusse *et al*, 2000; Coureux *et al*, 2003). (**B**) Seven hydrogen bonds interactions occur between the second-part of switch II and the L50 subdomain in the rigor-like state (and post-rigor states of other myosins). (**C**) All these interactions are lost in the myosin post-rigor structure. Instead, this region of switch II is closer to the nucleotide-binding elements, switch I and P-loop, and interacts with them in the myosin VI post-rigor structure. (**D**) While switch II remains close to the nucleotide-binding elements in the pre-powerstroke state, a movement of the L50 subdomain towards the nucleotide-binding site allows all the interactions between switch II and the L50 subdomain to reform in this state.

E461 interacts with a different arginine of switch I, R199. Thus, this unexpected conformation of switch II in the post-rigor state of myosin VI reveals that the second part of switch II can be more mobile than previously thought. This in turn could facilitate the formation of interactions between switch II and switch I, which is necessary to promote the rearrangements of the recovery stroke.

Discussion

We have solved the structure of myosin VI with the ATP analogue ADP.BeF_3 bound in its nucleotide-binding pocket. Based on the high degree of similarity of previously solved myosin structures (Figure 2; Table I), we have classified the structure as representing the post-rigor state of myosin VI. It is worth noting the fact that in the overall myosin ATPase cycle activated by actin, there are only two major biochemical states populated when myosin is detached from actin, the myosin.ATP state and the myosin.ADP.P_i state, which rapidly equilibrate (Holmes and Geeves, 2000). There is general consensus that the myosin.ATP state in solution is equivalent to the structural state (post-rigor state) seen with the ATP analogue ADP.BeF_3 bound, and that the myosin.ADP.P_i state is captured by crystals with either ADP.AlF_4 or ADP.VO_4, (pre-powerstroke state). Thus, two conformations of myosin have been seen with ATP analogues, and these undoubtedly correspond to the two steady state intermediates in the ATPase cycle that are populated in the absence of actin. In the absence of both actin and ATP or ATP analogues, myosin is not as constrained as it would be in the presence of actin, and thus may populate structural states that are not in the cycle.

The post-rigor structure of myosin VI reveals that the pathway of communication between the actin-binding site, the nucleotide-binding site and the lever arm allows detachment from F-actin upon ATP binding without a reverse stroke, as has been seen previously for plus-end myosin motors. As described for plus-end motors, the major element in this transition is the distortion of the transducer. An important difference in the myosin VI motor, however, is the ability of its converter to rearrange during the powerstroke. What is revealed with this new structure is that the myosin VI converter remains in the conformation found in the rigor-like state when it transitions to the post-rigor state, with maintenance of the interactions between the N-terminal subdomain and the converter, as found in the rigor-like state. This prevents a partial reversal of the powerstroke that would occur if the converter rearranged during the transition from rigor to post-rigor. The maintenance of the converter N-terminal interactions is made possible by a relative movement of the relay–converter interface, essentially a sliding on hydrophobic residues. Without this accommodation, the N-terminal interactions with the converter likely would have broken, destabilizing the rigor converter conformation, which in turn would move the lever arm in the repriming direction. Furthermore, during the subsequent recovery stroke, these adaptations, as well as alterations in the SH1-helix and the cavity surrounding it, may be critical to allow maintained connectivity between the relay and the converter while both the relay and the SH1-helix reposition and the converter undergoes its conformational change to form the pre-powerstroke structure.

Another interesting feature of the myosin VI post-rigor structure is an ~2.5-Å movement of switch II away from the L50 subdomain (Figure 6). This separation of switch II from the L50 domain has not been seen in any other myosin structure. It likely results from the substitution of what is normally an isoleucine in switch II of myosin I and II for a tyrosine (Y462). This tyrosine is too bulky to fit into the pocket where the isoleucine normally sits (occupied by a threonine in myosin V). This may tend to destabilize the switch II position in myosin VI. The fact that this substitution is conserved in all class VI myosins and is found in no other myosin class suggests that it is of functional significance.

In summary, in order to maximize the size of its powerstroke, myosin VI, like members of all other myosin classes, must minimize lever arm movement during the transition from rigor to post-rigor (i.e., detachment from actin). To accomplish this, myosin VI maintains the rigor conformation of its converter upon detachment from actin, which necessitates that the converter must maintain its interactions with the N-terminal subdomain. We speculate that this requires myosin VI to have increased flexibility in the interface

between the relay and converter. However, these adaptations that prevent converter rearrangement (and lever arm movement) during detachment from actin likely stabilize the post-rigor state. This would shift the hydrolysis equilibrium away from myosin.ADP.P_i and toward myosin.ATP by tending to slow the conversion to the pre-powerstroke conformation, which involves the recruitment of switch II for ATP hydrolysis. The previously unseen movement of switch II that occurs in the post-rigor state of myosin VI positions it closer to its pre-powerstroke position, and may facilitate its recruitment by the gamma-phosphate of ATP. In other words, the increased freedom of movement of this region of switch II relative to the L50 subdomain may aid in closing the cleft near the nucleotide pocket that is seen in the pre-powerstroke state by forming switch I–switch II interactions. The L50 subdomain would follow switch II, as bonds between the second part of switch II and the L50 subdomain reform. This movement of the L50 subdomain would cause the converter to break its interactions with the N-terminal subdomain. This in turn could trigger the rearrangement of the converter to its pre-powerstroke conformation, which would complete a complex recovery stroke, positioning the myosin VI lever arm for the next powerstroke. Thus, we propose that without the movement of switch II away from the L50 subdomain in the post-rigor state, hydrolysis of ATP would be slowed, which would decrease processivity of the myosin VI dimer.

Materials and methods

Protein constructs, expression and ATPase assays

To create the myosin VI construct used to obtain crystals, the porcine myosin VI cDNA was truncated after alanine 816. This truncation is at the end of insert 2 and precedes the CaM-binding IQ motif. From this construct, we removed insert 1 (ΔC278–A303), as previously described (Ménétrey *et al*, 2005). A Flag tag (encoding GDYKDDDDK) was appended to the N-terminus to allow for purification. This construct ($MD^{insert\ 2,}\ \Delta^{insert\ 1}$) was used to create recombinant baculovirus for expression in SF9 cells, as previously described (Sweeney *et al*, 1998). The myosin-expressing viruses were co-infected with a virus encoding chicken calmodulin, and the expressed calmodulin-containing myosin molecules were purified as previously described (Sweeney *et al*, 1998).

Crystallization and data collection

Crystals of myosin VI $MD^{insert\ 2,}\ \Delta^{insert\ 1}$ were obtained by vapor diffusion, with spontaneous nucleation occurring at 4°C in hanging drops, using equal amounts of reservoir solution (containing 8% PEG 8000, 50 mM glycine pH 9.5, 6% MPD) and stock solution of the protein at 13–16 mg/ml. Seeding was then used to improve crystal size and quality. Before freezing and data collection, the crystals were transferred in a two-step process into a final cryoprotectant solution containing 12% PEG 8000 with 25% MPD. X-ray data set were collected at 100 K on the ID23-1 and ID23-2 beamlines of the European Synchrotron Radiation Facility. Data sets were integrated with XDS (Kabsch, 1993) and scaled with SCALA (CCP4, 1994). The improved crystals diffract up to 2.4 Å, belong to the orthorhombic space group $P2_12_12_1$, with one molecule in the asymmetric unit and $a = 73.42$ Å, $b = 100.47$ Å and $c = 174.07$ Å cell parameters. See Table II for statistics on data collection.

Structural determination and refinement

The myosin VI structure was solved by molecular replacement with the program Phaser (McCoy *et al*, 2005), at 2.4-Å resolution using the rigor-like structure of myosin VI (PDB code 2BKH). Then, a rigid-body search was carried out with each of the myosin VI subdomains (SH3 motif, Nter, U50, L50, converter and the distal portion of insert 2 and its Ca^{2+}.CaM) with Refmac5 (CCP4, 1994). The overall refinement and water/heterogen molecule attribution were then carried out at 2.4-Å resolution with Refmac5 and Coot (Emsley and Cowtan, 2004). See Table II for statistics on structural refinement. Note that all figures were computed using MOLSCRIPT (Kraulis, 1991) and Pymol (DeLano, 2002).

Accession numbers

Atomic coordinates and structure factors have been deposited in the Protein Data Bank under the accession numbers 2VAS and r2vassf, respectively, for the post-rigor structure of the myosin VI motor domain.

Supplementary data

Supplementary data are available at *The EMBO Journal* Online (http://www.embojournal.org).

Acknowledgements

This work was supported by grants from NIAMS and NIDCD (HLS), the CNRS (AH), the ANR (AH) and the ACI BCMS (AH).

Conflict of interest

The authors declare that they have no competing financial interests.

References

Bryant Z, Altman D, Spudich JA (2007) The power stroke of myosin VI and the basis of reverse directionality. *Proc Natl Acad Sci USA* **104:** 772–777

Collaborative Computational Project Number 4 (1994) The CCP4 suite: program for protein crystallography. *Acta Crystallogr D* **50:** 760–763

Coureux PD, Sweeney HL, Houdusse A (2004) Three myosin V structures delineate essential features of chemo-mechanical transduction. *EMBO J* **23:** 4527–4537

Coureux PD, Wells AL, Ménétrey J, Yengo CM, Morris CA, Sweeney HL, Houdusse A (2003) A structural state of the myosin V motor without bound nucleotide. *Nature* **425:** 419–423

DeLano WL (2002) The PyMOL molecular graphics system. DeLano Scientific, San Carlos, CA www.pymol.org

Emsley P, Cowtan K (2004) Coot: model-building tools for molecular graphics. *Acta Crystallogr D* **60:** 2126–2132

Fischer S, Windshugel B, Horak D, Holmes KC, Smith JC (2005) Structural mechanism of the recovery stroke in the myosin molecular motor. *Proc Natl Acad Sci USA* **102:** 6873–6878

Fisher AJ, Smith CA, Thoden JB, Smith R, Sutoh K, Holden HM, Rayment I (1995) X-ray structures of the myosin motor domain of *Dictyostelium discoideum* complexed with MgADP.BeFx and MgADP.AlF4-. *Biochemistry* **34:** 8960–8972

Furch M, Fujita-Becker S, Geeves MA, Holmes KC, Manstein DJ (1999) Role of the salt-bridge between switch-1 and switch-2 of *Dictyostelium* myosin. *J Mol Biol* **290:** 797–809

Gulick AM, Bauer CB, Thoden JB, Rayment I (1997) X-ray structures of the MgADP, MgATPgammaS, and MgAMPPNP complexes of the *Dictyostelium discoideum* myosin motor domain. *Biochemistry* **36:** 11619–11628

Holmes KC, Geeves MA (2000) The structural basis of muscle contraction. *Philos Trans R Soc Lond B Biol Sci* **355:** 419–431

Houdusse A, Szent-Györgyi A, Cohen C (2000) Three conformational states of scallop myosin subfragment S1. *Proc Natl Acad Sci USA* **97:** 11238–11243

Kabsch W (1993) Automatic processing of rotation diffraction data from crystals of initially unknown symmetry and cell constants. *J Appl Cryst* **26:** 795–800

Koppole S, Smith JC, Fischer S (2006) Simulations of the myosin II motor reveal a nucleotide-state sensing element that controls the recovery stroke. *J Mol Biol* **361:** 604–616

Kraulis PJ (1991) MOLSCRIPT: a program to produce both detailed and schematic plots of protein structures. *J Appl Cryst* **24:** 946–950

McCoy AJ, Grosse-Kunstleve RW, Storoni LC, Read RJ (2005) Likelihood-enhanced fast translation functions. *Acta Crystallogr D* **61:** 458–464

Ménétrey J, Bahloul A, Wells AL, Yengo CM, Morris CA, Sweeney HL, Houdusse A (2005) The structure of the myosin VI motor reveals the mechanism of directionality reversal. *Nature* **435:** 779–785

Ménétrey J, Llinas P, Mukherjea M, Sweeney HL, Houdusse A (2007) The structural basis for the large powerstroke of myosin VI. *Cell* **131:** 300–308

Park H, Li A, Chen L-Q, Houdusse A, Selvin PR, Sweeney HL (2007) The unique insert at the end of the myosin VI motor is the sole determinant of directionality. *Proc Natl Acad Sci USA* **104:** 778–783

Rock RS, Ramamurthy B, Dunn AR, Beccafico S, Morris CA, Spink B, Rami B, Franzini-Armstrong C, Spudich JA, Sweeney HL (2005) A flexible domain is essential for the large step size and processivity of myosin VI. *Mol Cell* **17:** 603–609

Sweeney HL, Houdusse A (2004) The motor mechanism of myosin V: insights for muscle contraction. *Philos Trans R Soc Lond B Biol Sci* **359:** 1829–1841

Sweeney HL, Houdusse A (2007) What can myosin VI do in cells? *Curr Opin Cell Biol* **19:** 57–66

Sweeney HL, Park H, Zong AB, Yang Z, Selvin PR, Rosenfeld SS (2007) How myosin VI coordinates its heads during processive movement. *EMBO J* **26:** 2682–2692

Sweeney HL, Rosenfeld SS, Brown F, Faust L, Smith J, Stein L, Sellers J (1998) Kinetic tuning of myosin via a flexible loop adjacent to the nucleotide-binding pocket. *J Biol Chem* **273:** 6262–6270

Wells AL, Lin AW, Chen L-Q, Safer D, Cain SM, Hasson T, Carragher BO, Milligan RA, Sweeney HL (1999) Myosin VI is an actin-based motor that moves backwards. *Nature* **401:** 505–508

Yang Y, Gourinath S, Kovacs M, Nyitray L, Reutzel R, Himmel DM, O'neall-Hennessey E, Reshetnikova L, Szent-Gyorgyi AG, Brown JH, Cohen C (2007) Rigor-like structures from muscle myosins reveal key mechanical elements in the transduction pathways of this allosteric motor. *Structure* **15:** 553–564

